

# Peroxisome Proliferator-activated Receptors and Hepatic Stellate Cell Activation\*

Received for publication, July 24, 2000

Published, JBC Papers in Press, August 31, 2000, DOI 10.1074/jbc.M006577200

Takeo Miyahara,<sup>a</sup> Laura Schrum,<sup>e</sup> Richard Rippe,<sup>d</sup> Shigang Xiong,<sup>a</sup> Hal F. Yee, Jr.,<sup>f</sup> Kenta Motomura,<sup>a</sup> Frank A. Anania,<sup>g</sup> Timothy M. Willson,<sup>h</sup> and Hidekazu Tsukamoto,<sup>a,b,c</sup>

From the Departments of <sup>a</sup>Medicine and <sup>b</sup>Pathology, Keck School of Medicine of the University of Southern California, Los Angeles, California 90033, <sup>c</sup>Department of Veterans Affairs Greater Los Angeles Healthcare System, Sepulveda, California 91343, Departments of <sup>d</sup>Medicine and <sup>e</sup>Surgery, University of North Carolina, Chapel Hill, North Carolina 27599-7038, <sup>f</sup>Departments of Medicine and Physiology, University of California, Los Angeles, California 90095, <sup>g</sup>Department of Medicine, University of Maryland, College Park, Maryland 21201, <sup>h</sup>Department of Medicinal Chemistry, Glaxo Wellcome Research and Development, Research Triangle Park, North Carolina 27709-3398

The present study examined the roles of peroxisome proliferator-activated receptors (PPAR) in activation of hepatic stellate cells (HSC), a pivotal event in liver fibrogenesis. RNase protection assay detected mRNA for PPAR $\gamma$ 1 but not that for the adipocyte-specific  $\gamma$ 2 isoform in HSC isolated from sham-operated rats, whereas the transcripts for neither isoforms were detectable in HSC from cholestatic liver fibrosis induced by bile duct ligation (BDL). Semi-quantitative reverse transcriptase-polymerase chain reaction confirmed a 70% reduction in PPAR $\gamma$  mRNA level in HSC from BDL. Nuclear extracts from BDL cells showed an expected diminution of binding to PPAR-responsive element, whereas NF- $\kappa$ B and AP-1 binding were increased. Treatment of cultured-activated HSC with ligands for PPAR $\gamma$  (10  $\mu$ M 15-deoxy- $\Delta^{12,14}$ -PGJ<sub>2</sub> (15dPGJ<sub>2</sub>); 0.1–10  $\mu$ M BRL49653) inhibited DNA and collagen synthesis without affecting the cell viability. Suppression of HSC collagen by 15dPGJ<sub>2</sub> was abrogated 70% by the concomitant treatment with a PPAR $\gamma$  antagonist (GW9662). HSC DNA and collagen synthesis were inhibited by WY14643 at the concentrations known to activate both PPAR $\alpha$  and  $\gamma$  (>100  $\mu$ M) but not at those that only activate PPAR $\alpha$  (<10  $\mu$ M) or by a synthetic PPAR $\alpha$ -selective agonist (GW9578). 15dPGJ<sub>2</sub> reduced  $\alpha$ 1(I) procollagen, smooth muscle  $\alpha$ -actin, and monocyte chemoattractant protein-1 mRNA levels while inducing matrix metalloproteinase-3 and CD36. 15dPGJ<sub>2</sub> and BRL49653 inhibited  $\alpha$ 1(I) procollagen promoter activity. Tumor necrosis factor  $\alpha$  (10 ng/ml) reduced PPAR $\gamma$  mRNA, and this effect was prevented by the treatment with 15dPGJ<sub>2</sub>. These results demonstrate that HSC activation is associated with the reductions in PPAR $\gamma$  expression and PPAR-responsive element binding *in vivo* and is reversed by the treatment with PPAR $\gamma$  ligands *in vitro*. These findings implicate diminished

PPAR $\gamma$  signaling in molecular mechanisms underlying activation of HSC in liver fibrogenesis and the potential therapeutic value of PPAR $\gamma$  ligands for liver fibrosis.

Hepatic stellate cells (HSC)<sup>1</sup> are vitamin A-storing, perisinusoidal pericytes that serve as the major source of extracellular matrices in liver fibrosis (1). The most intriguing aspect of the involvement of HSC in liver fibrogenesis is that HSC undergo phenotypic changes often characterized as “myofibroblastic activation” (1–3). During this activation, HSC lose their intracellular vitamin A content (4, 5), induce MMP-2 and -3 to facilitate matrix remodeling (6, 7), proliferate (8, 9), up-regulate expression of matrix proteins (10, 11), tissue inhibitors of metalloproteinase (TIMP) (12),  $\alpha$ -smooth muscle actin (5, 13), and endothelin receptors (14, 15), and undergo actin cytoskeleton-dependent alterations in morphology (16).

To understand the molecular basis of the multifaceted cellular changes in HSC activation, increasing efforts have been made to characterize alterations in specific gene regulation or intracellular signaling that may confer some of the activation events. Such examples include up-regulation of autocrine cytokines such as TGF- $\beta$  (5, 8, 11), TGF- $\alpha$  (8), interleukin-10 (17), and their receptors (18, 19). In particular, the evidence for the pivotal role of TGF- $\beta$  in liver fibrogenesis is compelling, as exemplified by a recent demonstration of amelioration of experimental liver fibrosis by an adenovirus vector expressing the dominant negative TGF- $\beta$  type II receptor (20). Early genes induced during activation of HSC may be associated with induction of this fibrogenic cytokine. One such example is a Kruppel-like zinc finger transcription factor, Zf9, which was recently shown to transactivate promoters for both TGF- $\beta$ 1 and type I and II TGF- $\beta$  receptors (21). Alternatively, the changes in the cellular content of retinoids may favor induction of TGF- $\beta$ . Depletion of retinoids occurs in activation of HSC both in culture (4) and *in vivo* (5) and appears to precede induction of TGF- $\beta$ 1 and matrix genes (5). All-*trans* and 9-*cis* retinoic acids (RA), biologically active metabolites of vitamin A, are also

\* This study was supported by National Institutes of Health Grants R37-AA06603 (to H. T.), DK02450 (to H. Y.), DR34987 (to R. P.), and AA10459 (to R. P.), University of Southern California-UCLA Research Center for Alcoholic Liver and Pancreatic Diseases Grant P50-AA11999, Molecular Biology and Tissue Culture Core facilities of University of Southern California Research Center for Liver Diseases Grant P30-DK48522, and a grant from the Medical Research Service of the Department of Veterans Affairs (to H. T.). The costs of publication of this article were defrayed in part by the payment of page charges. This article must therefore be hereby marked “advertisement” in accordance with 18 U.S.C. Section 1734 solely to indicate this fact.

<sup>1</sup> To whom correspondence should be addressed: Keck School of Medicine, University of Southern California, 1333 San Pablo St., MMR-412, Los Angeles, CA 90033. Tel.: 323-442-5107; Fax: 323-442-3126; E-mail: htsukamo@hsc.usc.edu.

<sup>1</sup> The abbreviations used are: HSC, hepatic stellate cells; PPAR, peroxisome proliferator-activated receptor; RA, retinoic acid; RAR, retinoic acid receptor; RXR, retinoid X receptor; MCP-1, monocyte chemoattractant protein-1; PPRE, peroxisome proliferator-activated receptor response element; TNF $\alpha$ , tumor necrosis factor  $\alpha$ ; MMP, matrix metalloproteinase; TGF, transforming growth factor; AP-1, activator protein-1; NF- $\kappa$ B, nuclear factor  $\kappa$ B; RT-PCR, reverse transcription-polymerase chain reaction; 15dPGJ<sub>2</sub>, 15-deoxy- $\Delta^{12,14}$ -PGJ<sub>2</sub>; BDL, bile duct ligation;  $\alpha$ -SMA, smooth muscle  $\alpha$ -actin; aP2, adipocyte fatty acid binding protein.

depleted in activated HSC isolated from experimental biliary liver fibrosis (22). RAR and RXR serve as nuclear receptors for RA, and their levels are also reduced in activated HSC (22). RAR and RXR are known to antagonize AP-1 promoter activities of TGF- $\beta$ 1 (23) and metalloproteinases (24, 25) in a RA-dependent manner. Thus, it is plausible that deficiencies of RA, RAR, and RXR may permissively up-regulate AP-1 activity in activated HSC via suppressed RA-mediated, negative cross-coupling of this transcription factor. In fact the treatment of cultured HSC with all-*trans* RA causes suppression of cell proliferation, collagen, and TGF- $\beta$  production (26). On the contrary, 9-*cis* RA (27) and 9,13-di-*cis*-RA (28) are shown to activate latent TGF- $\beta$  via up-regulation of tissue plasminogen activator. These conflicting effects may be due to the recently demonstrated differential effects of the RA isomers on HSC (29) or complex responses rendered by RA, particularly via RXR.

RXR heterodimerizes with the members of the steroid/thyroid hormone receptor superfamily, such as vitamin D receptor, thyroid hormone receptor, peroxisome proliferator-activated receptor (PPAR), liver X receptor (LXR), and farnesoid X-activated receptor (FXR) (30). Since RXR serves as a ligand-dependent, active partner for some of these receptors such as PPAR and LXR, the reduced levels of 9-*cis* RA and RXR, as previously shown by us in HSC from cholestatic livers (22), may limit activities of the transcription factors. In particular, we hypothesized whether PPAR $\gamma$  expression might be suppressed in activated HSC. This hypothesis was inspired by the recent demonstration of leptin induction in culture-activated HSC (31). Leptin, a 16-kDa protein most exclusively expressed in adipose tissue, is the product of the *ob* gene, which suppresses food intake, increases metabolic rate, and reduces fat depot size (See Ref. 32 for review). The deficiency of leptin or its receptor is associated with the obesity in mice and human. Thus, the finding that leptin expression is induced in culture-activated HSC suggests the possibility that HSC may share the adipocyte phenotype. In fact, quiescent HSC is characterized by ample intracellular storage of lipids including fat-soluble vitamin A, and activation of HSC causes depletion of lipid droplets and transdifferentiation to myofibroblastic phenotype. These changes resemble transdifferentiation of 3T3-L1 cells that possess the potential to differentiate into either fibroblasts (preadipocytes) or adipocytes. With appropriate stimulation with fetal calf serum, dexamethasone, insulin, etc., 3T3-L1 cells undergo adipocyte differentiation driven by transcription factors such as PPAR $\gamma$ , C/EBP, and ADD1/SREBP1(32). Conversely, suppressed activities of these transcription factors result in fibroblastic differentiation (32).

In the present study, we have examined expression of PPAR $\gamma$  isoforms in quiescent HSC isolated from normal rats and activated HSC from experimental biliary liver fibrosis. RNase protection assay revealed expression of  $\gamma$ 1 isoform in quiescent HSC but not that of the adipocyte-specific  $\gamma$ 2 form, providing no support to the hypothesis that HSC share the adipogenic phenotype. However, we disclosed marked reductions in expression of PPAR $\gamma$  and PPAR response element (PPRE) binding in the *in vivo* activated HSC. Furthermore, the treatment of culture-activated HSC with PPAR $\gamma$  ligands (15dPGJ<sub>2</sub> and BRL49653) reversed biochemical features of HSC activation. In particular, the ligands inhibited  $\alpha$ 1(I) procollagen promoter activity, its mRNA expression, and collagen production by the cells, and the inhibition by 15dPGJ<sub>2</sub> was shown to be blocked by a PPAR $\gamma$  antagonist, confirming the involvement of PPAR $\gamma$ . These results suggest the pivotal roles of PPAR $\gamma$  in molecular regulation of HSC activation in liver fibrogenesis.

## MATERIALS AND METHODS

**Bile Duct Ligation**—Bile duct ligation was performed using male Wistar rats weighing 550–650 g by aseptic ligation and scission of the common bile duct (BDL) as described previously (22). Another group of rats was sham-operated by exposing the common bile duct without ligation or scission as a control (sham). The animal protocol in this study was approved by the Institutional Care and Use Committee of the University of Southern California.

**HSC Isolation**—Hepatic stellate cells were isolated from BDL, sham, and normal rats by the method previously described (5, 22). Briefly, the liver was perfused *in situ* first with calcium-free minimum essential medium (Life Technologies, Inc.) followed by 0.62% Pronase (Roche Molecular Biochemicals) and 0.0125% type IV collagenase (Sigma) in Dulbecco's modified Eagle's medium/F-12 (Life Technologies, Inc.). For rats cholestatic for 19 days, a mixture of 0.02% type IV collagenase and 0.04% type I collagenase (Roche Molecular Biochemicals) was used because of the extremely fibrotic condition of the livers. The liver was carefully removed and minced with scissors. The digested liver was further incubated in a shaker-incubator with 0.035% pronase and 62.5 units/ml DNase (Sigma) in Dulbecco's modified Eagle's medium/F-12 at 37 °C for 30 min. It was then filtered through gauze, and parenchymal cells were removed by low speed centrifugation. The resultant supernatant was laid on top of the four density gradients (1.035, 1.045, 1.058, and 1.085) of arabinogalactan (LARCOLL, Sigma) and centrifuged at 21,400 rpm for 45 min at 25 °C using Beckman SW41-Ti rotor (Beckman Instruments). The interface between the media and the density 1.035 was recovered as a pure HSC fraction. The purity of isolated HSC were examined by phase contrast microscopy and ultraviolet-excited fluorescence microscopy and the viability by trypan blue exclusion.

**Primary Culture of HSC**—Isolated HSC from normal rats were cultured in six-well plates with RPMI 1640 supplemented with 10% fetal bovine serum, 100 units/ml streptomycin, and 100 units/ml penicillin and amphotericin B (Life Technologies, Inc.). The cultures were maintained for 3–4 days or 6–7 days before tested for effects of PPAR ligands. By these time points the cells began to show or already showed morphological features of culture-activated HSC as described previously (1, 13). For DNA and collagen synthesis analyses, HSC were seeded in 24-well plates with the aforementioned media. For morphological examination of HSC, the cells were cultured onto 10-mm<sup>2</sup> coverslips placed in 6-well plates for 7 days before testing the effects of 15dPGJ<sub>2</sub> or BRL49653. To assess the effects of PPAR $\alpha$  and PPAR $\gamma$  ligands on HSC *in vitro*, cultured HSC were washed twice with phosphate-buffered saline and incubated in serum-free media. The cells were then treated with 15dPGJ<sub>2</sub> (1–10  $\mu$ M, Biomol, Plymouth Meeting, PA), BRL49653 (0.1–10  $\mu$ M, a gift from Glaxo Wellcome, Research Triangle Park, NC), or WY14643 (1–250  $\mu$ M, Biomol) or vehicle alone (Me<sub>2</sub>SO for WY14643 and BRL49653 or ethanol for 15dPGJ<sub>2</sub>) for 18 h. These cells were examined for DNA and collagen synthesis, morphological analysis, and mRNA expression for various activation maker genes as described below. To test the PPAR $\gamma$  dependence of 15dPGJ<sub>2</sub>-mediated effect on HSC collagen synthesis, the cells were concomitantly incubated with a PPAR $\gamma$  antagonist, GW9662 (33, 34).

**DNA and Collagen Synthesis**—DNA synthesis was determined as incorporation of [<sup>3</sup>H]thymidine (10  $\mu$ Ci/ml) into HSC DNA as described previously (9). Collagen synthesis was determined by incorporation of [<sup>3</sup>H]proline (10  $\mu$ Ci/ml) into collagenase-sensitive peptides in the presence of ascorbic acid (50  $\mu$ g/ml) and  $\beta$ -aminopropionitrile fumarate (50  $\mu$ g/ml) as described (17).

**RNA and Nuclear Protein Extraction**—Total RNA was extracted from isolated HSC by the guanidinium-phenol-chloroform method of Chomczynski and Sacchi (35) and nuclear protein by the method of Schreiber *et al.* (36). RNA and nuclear protein concentrations were determined by the absorbance at 260 nm and a Bradford assay, respectively.

**RNase Protection Assay and Reverse Transcription-PCR**—RNase protection assay was performed for PPAR $\gamma$ 1 and - $\gamma$ 2 transcripts using an approach previously described (37). A partial PPAR $\gamma$  cDNA was generated by RT-PCR using the rat PPAR $\gamma$ 2-specific primers, which amplified a region that includes 90 base pairs of the PPAR $\gamma$ 2 transcript and 185 base pairs common to both PPAR $\gamma$ 1 and  $\gamma$ 2. The cDNA was ligated into the PGEM-3 vector for generation of an antisense RNA probe. The assay was performed using <sup>32</sup>P-labeled RNA probe, 5 or 10  $\mu$ g of RNA from HSC isolated from BDL and sham, and a RNase protection assay kit from Torrey Pines Biolabs, Inc. (San Diego, CA). As a control, L32 was used. For RT-PCR analysis for HSC activation marker genes, 2  $\mu$ g of total RNA was transcribed into cDNA using 600



units of Moloney murine leukemia virus reverse transcriptase and oligo(dT)<sub>15</sub> as a primer at 37 °C for 60 min. The synthesized cDNA were amplified using specific sets of primers for PPAR $\alpha$ , (CCTTTTGTGGCTGCTAT, TCCCTGCTCTCCTGTATG), PPAR $\gamma$  (ATTCTGGCCACC-AACTTCGG, TGGAAAGCCTGATGCTTTATCCCCA), smooth muscle  $\alpha$ -actin ( $\alpha$ -SMA) (TGTGCTGGACTCTGGAGATG, GATCACCTGCCA-TCAGG),  $\alpha$ 1(I) procollagen (17), MMP-3 (ACGCACAACCTCAAGCTG-CC, TTAATTCGGAAGACGCCAGAAC), MMP-13 (17), MCP-1 (GAAC-CAGGATTCACAGAG, ATGCAGGTATATGTCACGC), CD-36 (GGAG-GCATTCTCATGCCGGTTGGAG, TGAGAACTGTGAAGTTGTCATTCTC), and  $\beta$ -actin (22). Each PCR mixture contained 0.4  $\mu$ M of a set of specific primers, 0.2  $\mu$ M each dNTP, 2.5 units *Taq* polymerase, 1.5  $\mu$ M MgCl<sub>2</sub>, and 2  $\mu$ l of cDNA except for  $\beta$ -actin, for which 1  $\mu$ l was used. PCR procedure consisted of 20 cycles ( $\alpha$ -SMA,  $\alpha$ 1(I) procollagen, MCP-1, and  $\beta$ -actin) or 30–35 cycles (PPAR $\alpha$ , PPAR $\gamma$ , MMP-3, and MMP-13) of denaturation at 94 °C for 45 s, annealing at 55 °C for 30 s, extension at 72 °C for 90 s, with initial denaturation of sample cDNA at 94 °C for 3 min before PCR and additional extension period of 10 min after the last cycle. PCR products were run on 1.5% agarose gel containing 0.004% ethidium bromide and visualized under UV transilluminator. The densitometric analysis of PCR products was performed by the computer software, ImageQuant for Power Macintosh v1.2 (Molecular Dynamics), and standardized by the  $\beta$ -actin.

**Electrophoretic Mobility Shift Assay**—Nuclear protein extract (10–20  $\mu$ g) was incubated with a reaction mixture (20 mM HEPES, pH 7.6, 100 mM KCl, 0.2 mM EDTA, 2 mM dithiothreitol, 20% glycerol, 200  $\mu$ g/ml poly(dI-dC)) on ice for 10 min. One to two ng of a <sup>32</sup>P-labeled double-stranded ARE-7 (PPRE) (38), AP-1 (22), or NF- $\kappa$ B (39) oligonucleotides were added and incubated for an additional 20 min. The reaction mixture was then resolved on a 6% nondenaturing polyacrylamide gel in 0.5 $\times$  TBE (45 mM Tris, 45 mM boric acid, 1 mM EDTA). The gel was dried and subjected to autoradiography at –80 °C. For supershift assay, we have used antisera against PPAR $\gamma$  (kindly provided by Dr. Ronald M. Evans, The Salk Institute, San Diego, CA) and polyclonal antibodies against P65, P50, c-Fos, and c-Jun (Santa Cruz Biotechnology, Santa Cruz, CA).

**Transfection and Reporter Gene Assay**—To examine whether PPAR $\alpha$  and  $\gamma$  ligands have effects on collagen gene promoter activity, cultured HSC after the first passage were co-transfected with a collagen reporter gene plasmid (pGLCO2) that contains 2,200 base pairs of the murine  $\alpha$ 1(I) collagen gene 5'-flanking region ligand to the luciferase reporter gene (40) and a PPAR $\gamma$  expression vector (kindly provided by Dr. Ron Evans, The Salk Institute, San Diego, CA and Dr. Henry Sucov, Institute for Genetic Medicine, University of Southern California, Los Angeles, CA). The cells were serum-starved (0.2% fetal calf serum, 24 h) and then treated with 15dPGJ<sub>2</sub> (1 and 10  $\mu$ M), BRL49653 (10  $\mu$ M) for 24 h before their lysate was collected for luciferase assay. Liposomes were prepared using 1  $\mu$ g of the reporter gene plasmid and 2  $\mu$ g of the expression vector along with LipofectAMINE reagent (Life Technologies, Inc.). The cells were incubated with the liposomes for 3 h, the liposome mixture was removed, and fresh medium containing 10% fetal calf serum was added for incubation for 15 h.

**Morphological Analysis**—To investigate the effects of PPAR $\gamma$  ligand on the actin cytoskeleton and HSC morphology, cells cultured onto glass coverslips were exposed to 15dPGJ<sub>2</sub> (1 and 10  $\mu$ M) BRL49653 (1 and 10  $\mu$ M), or carrier (ethanol). Actin stress fibers and focal adhesion complexes were stained, and differential interference contrast images were acquired as described previously (16). Briefly, stress fibers were labeled with rhodamine-phalloidin, which binds to filamentous actin with high specificity. Focal adhesion complexes were labeled with an antibody directed against vinculin, a prominent component of the complex. A fluorescein-labeled secondary antibody was used to stain the focal adhesion complexes. Standard rhodamine and fluorescein filters (Chroma, Brattleboro, VT) were employed. Epifluorescence and differential interference contrast images were acquired digitally. The morphological analysis was performed by a blinded observer.

**Staining for Necrosis and Apoptosis**—To assess the effects of PPAR ligands on cultured HSC viability, we performed SYTOX<sup>®</sup> green nucleic acid staining (Molecular Probes, Inc. Eugene, OR) for necrosis and Hoechst staining (Sigma) for apoptosis. HSC were cultured in 24-well plates, treated with 15dPGJ<sub>2</sub> (1–10  $\mu$ M), BRL49653 (0.1–10  $\mu$ M), or WY14643 (100–250  $\mu$ M) for 18 h from day 6 to day 7 of primary cultures, washed gently with phosphate-buffered saline, and stained according to the manufacturer's suggested protocols. Two hundred cells were analyzed in triplicates, and the incidence of necrosis and apoptosis was expressed as the percentage of total cells examined.

**Statistical Analysis**—All data are expressed as means  $\pm$  S.E. The

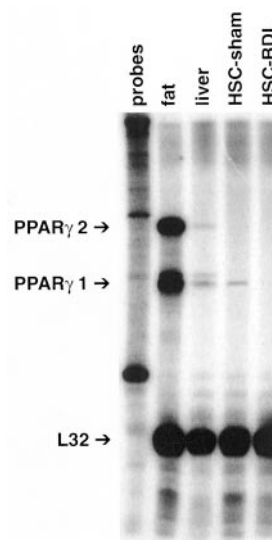


**FIG. 1. RNase protection assay for PPAR $\gamma$ 1 and  $\gamma$ 2 transcripts.** RNase protection assay was performed on samples (5  $\mu$ g each) extracted from rat epididymal fat (first lane), rat liver (third lane), hepatic stellate cells isolated from a sham-operated rat (HSC-sham, fourth lane), and hepatic stellate cells from a 7-day bile duct-ligated rat (HSC-BDL, fifth lane). Note the abundant expression of both forms of PPAR $\gamma$  in the fat sample. Even though the level of expression is much less, the liver RNA also contains both forms of PPAR $\gamma$ . However, only the PPAR $\gamma$ 1 transcript, but not an adipocyte specific PPAR $\gamma$ 2, is detected in the RNA sample from HSC-sham, and the PPAR $\gamma$ 1 expression is diminished in HSC-BDL.

significance for the difference between the groups was assessed using Student's *t* test.

## RESULTS

**PPAR $\gamma$  Isoform Expression by HSC**—Using a sensitive RNase protection assay that allowed simultaneous quantification of mRNA for both isoforms (37), we first examined expression of PPAR $\gamma$  isoforms in freshly isolated normal and *in vivo* activated HSC. As shown in Fig. 1, the assay detected abundant expression of both  $\gamma$ 2 and  $\gamma$ 1 isoforms in RNA extracted from rat epididymal fat (second lane). Liver tissue also expressed both isoforms but at much less levels (third lane). HSC isolated from sham-operated rats, expressed only  $\gamma$ 1 mRNA (fourth lane), and neither  $\gamma$ 1 nor  $\gamma$ 2 isoform was detectable in HSC from 1-week BDL animals (fifth lane). We also tested up to 10  $\mu$ g of RNA for HSC from sham and BDL rats with basically same results. Thus, these data demonstrated that normal rat HSC express  $\gamma$ 1 mRNA, the isoform that is generally expressed in various tissues (37), but not the  $\gamma$ 2 isoform, which is more selectively expressed in adipocytes. Furthermore, HSC from experimental biliary liver fibrosis (BDL) appeared to be depleted of PPAR $\gamma$ 1 expression.

**Diminished PPAR Expression by *in Vivo* Activated HSC**—Since the RNase protection assay failed to detect PPAR $\gamma$  transcripts in HSC from 1-week BDL, we next performed RT-PCR to amplify the mRNA. This PCR did not distinguish the isoforms and amplified both. After 35 cycles, we were able to detect PPAR $\gamma$  in HSC from BDL. However, the level of PPAR $\gamma$  expression was reduced as compared with HSC from sham, whereas mRNA expression for  $\alpha$ 1(I) collagen and  $\alpha$ -SMA was induced (Fig. 2A). Next, we examined HSC from BDL rats at 19 days after the surgery. Similarly, the PPAR $\gamma$  level was conspicuously reduced in BDL animals (Fig. 2B). In addition, PPAR $\alpha$  mRNA level was also decreased in these animals (Fig. 2B). Semi-quantitative analysis of the PCR densitometric data revealed approximately 70–80% reduction in PPAR $\alpha$  and PPAR $\gamma$  mRNA expression in HSC from the 19-day BDL animals (Fig. 2C).

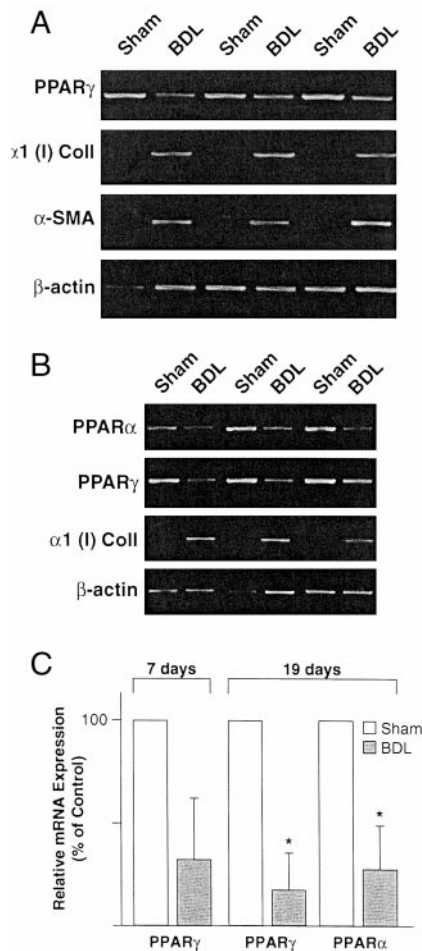


**FIG. 2.** A, PPAR $\gamma$  mRNA is reduced in HSC from 7-day BDL animals. RT-PCR demonstrates moderately reduced mRNA expression of PPAR $\gamma$  in HSC from the 7-day BDL animals, whereas induction of activation marker genes such as  $\alpha 1(I)$  procollagen ( $\alpha 1(I)$  *Coll*) and  $\alpha$ -SMA are evident in these cells. B, both PPAR $\alpha$  and PPAR $\gamma$  are suppressed in HSC from 19-day BDL animals. RT-PCR was performed as above on HSC RNA samples from rats 19 days after sham or BDL operation. Note the consistent reduction in the mRNA level of PPAR $\alpha$  and PPAR $\gamma$  in HSC from BDL animals. C, semi-quantitative densitometric analysis of the RT-PCR data depicting significantly (\*,  $p < 0.05$ ) decreased mRNA levels of PPAR $\alpha$  and PPAR $\gamma$  in HSC from 19-day BDL animals.

**Reduced PPARE Binding in HSC from BDL Animals**—To assess the consequence of the observed depletion of PPAR $\gamma$  and  $\alpha$ -mRNA levels, nuclear extracts were prepared from HSC from 19-day BDL and sham animals, and electrophoretic mobility shift assay was performed for PPARE binding. For this assay, we selected an ARE-7 probe (PPRE from aP2 gene) that preferentially binds PPAR $\gamma$  over PPAR $\alpha$  (38). As shown in Fig. 3, PPARE binding was appreciably decreased in HSC from BDL (*upper panel*). The specificity of this binding was supported by competition with  $\times 500$  excess cold probe (data not shown) and a supershift assay using antibodies against PPAR $\gamma$ . The latter technique demonstrated a diminution of the DNA binding with sham nuclear extracts and the appearance of a supershifted band (*arrow*, last lane, Fig. 3, *upper panel*), whereas non-immune serum did not affect the PPAR binding (data not shown). In contrast, NF- $\kappa$ B and AP-1 binding by the nuclear extracts from BDL HSC were conspicuously increased (*lower panels*). The specificity of NF- $\kappa$ B and AP-1 binding was supported by competition with excessive cold probe as well as supershift assays (data not shown), as previously performed in our laboratory (22, 39). Thus, these results demonstrate that “activated” HSC from the cholestatic liver fibrosis model are

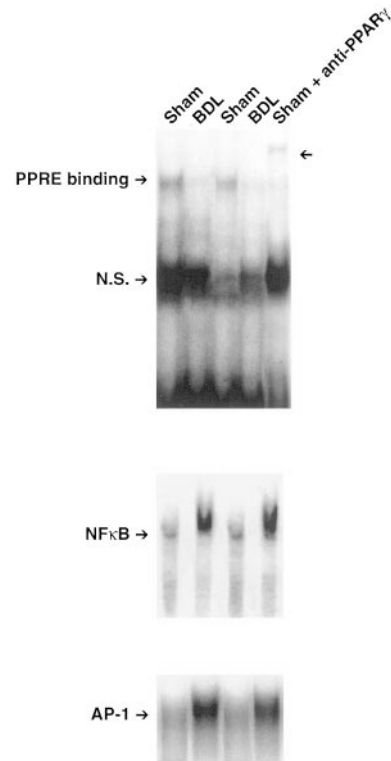


**FIG. 3.** PPARE binding is diminished in HSC from 19-day BDL animals. Nuclear extracts (10  $\mu$ g of protein per sample) from HSC isolated from 19-day sham or BDL animals were analyzed by electrophoretic mobility shift assay for binding to PPARE, NF- $\kappa$ B, or AP-1 site as described under “Materials and Methods.” Note PPARE binding is diminished in HSC from BDL animals, whereas NF- $\kappa$ B and AP-1 binding are enhanced. The last lane of the *upper panel* shows a supershift assay with anti-PPAR $\gamma$  antibodies, resulting in diminution of the binding by the sham HSC nuclear extracts and the appearance of a supershifted band (*arrow*). The use of non-immune antibodies did not affect the binding pattern (data now shown N.S. refers to nonspecific binding).

depleted of PPAR $\alpha$  and  $\gamma$  mRNA and PPARE binding and suggest the potential significance of these changes in activation of HSC.

**Effects of PPAR Ligands on HSC Viability in Culture**—To test the potential role of PPAR in regulating activation of HSC, we next investigated the *in vitro* effects of PPAR ligands on culture-activated HSC. For these experiments, we first examined the effects of PPAR ligands on HSC viability. We tested the ranges of 15dPGJ $_2$  (1–10  $\mu$ M), BRL49653 (0.1–10  $\mu$ M), and WY14643 (1–250  $\mu$ M) concentrations that had been used in earlier studies on other cell types (41–44). Staining of the cells for necrosis (SYTOX green nucleic acid staining) or apoptosis (Hoechst staining) showed no induction of either form of cell death by incubating the cells with these concentrations of 15dPGJ $_2$ , BRL49653, or WY14643 for 24 h. However, we observed a significant increase in the incidence of cell necrosis to  $6.90 \pm 2.75\%$  in the cells treated with 100  $\mu$ M 15dPGJ $_2$  as compared with  $0.83 \pm 0.29\%$  in the vehicle (ethanol)-treated cells. Based on these results, we used the non-cytotoxic concentrations of 15dPGJ $_2$  (1 and 10  $\mu$ M), BRL49653 (0.1–10  $\mu$ M), and WY14643 (10, 100, and 250  $\mu$ M) in the subsequent biochemical experiments.

**Effects of PPAR Ligands on HSC DNA and Collagen Synthesis**—We first examined the effects of PPAR $\gamma$  (15dPGJ $_2$  and BRL49653) and PPAR $\alpha$  (WY14643) ligands on DNA and collagen synthesis by cultured HSC. 15dPGJ $_2$  (10  $\mu$ M), BRL49653 (10  $\mu$ M), and WY14643 (250  $\mu$ M) caused 40% inhibition in HSC DNA synthesis (Fig. 4A). Collagen production as determined by [ $^3$ H]proline incorporation into collagenase-sensitive peptides

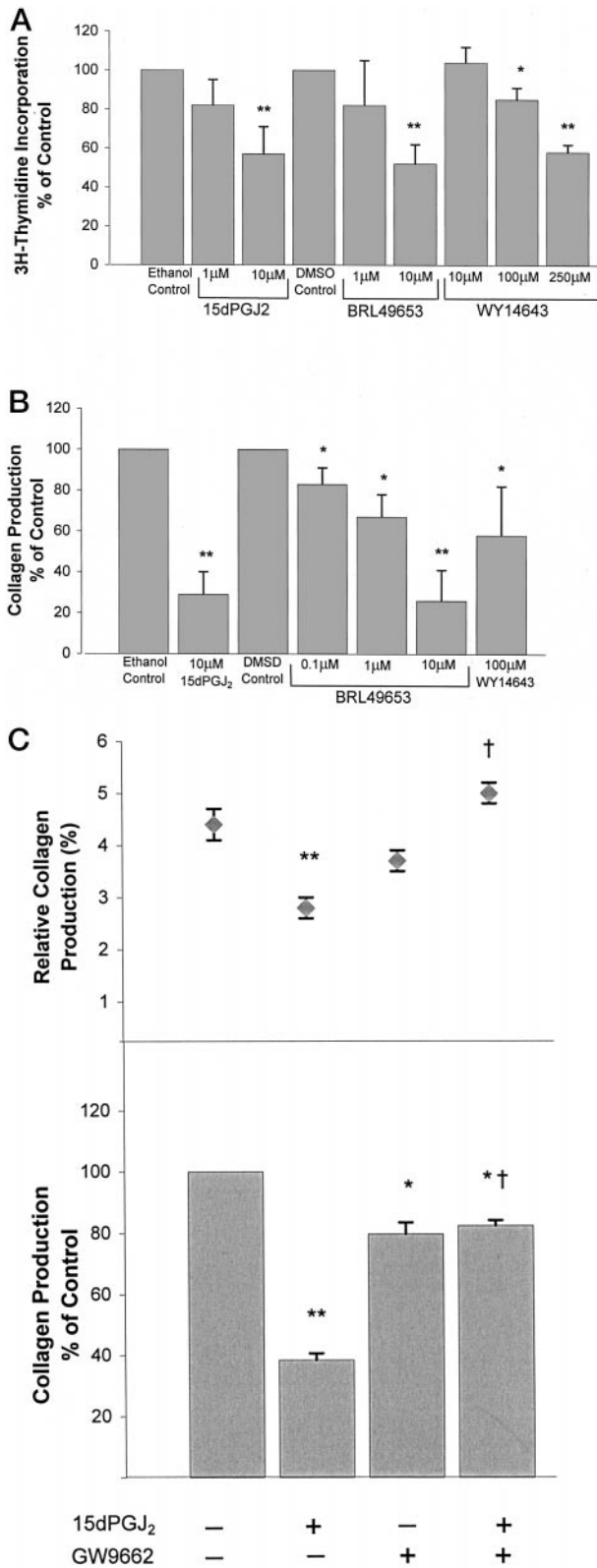


FIG. 4. A, PPAR $\gamma$  (15dPGJ<sub>2</sub>, BRL49653) ligands inhibit HSC DNA and collagen synthesis. The 3–4-day primary cultures of HSC were exposed to 15dPGJ<sub>2</sub> (1 and 10  $\mu$ M), BRL49653 (1 and 10  $\mu$ M), or WY14643 (10–250  $\mu$ M) for 18 h, and [<sup>3</sup>H]thymidine incorporation into DNA was assessed. Note a significant, ~40%, inhibition in HSC DNA synthesis by 15dPGJ<sub>2</sub> and BRL49653 at 10  $\mu$ M and WY14643 at 100 and 250  $\mu$ M. \*,  $p < 0.05$ ; \*\*,  $p < 0.01$  compared with the respective control. DMSO, Me<sub>2</sub>SO. B, collagen production by cultured HSC, as determined by incorporation of [<sup>3</sup>H]proline into collagenase-sensitive peptides was significantly inhibited by 18 h of treatment with 15dPGJ<sub>2</sub> (10  $\mu$ M), BRL49653 (0.1–10  $\mu$ M), and WY14643 (100  $\mu$ M). \*,  $p < 0.05$ ; \*\*,  $p < 0.01$ .

was also inhibited 75% by 15dPGJ<sub>2</sub> or BRL49653 (10  $\mu$ M) and 45% by WY14643 at 100  $\mu$ M (Fig. 4B). The inhibition by BRL49653 was also shown to be dose-dependent. Furthermore, the involvement of PPAR $\gamma$  in 15dPGJ<sub>2</sub>-mediated inhibition of collagen production was supported by prevention of the 15dPGJ<sub>2</sub> effect by a PPAR antagonist (GW9662) (Fig. 4C, lower panel). As shown in the upper panel of Fig. 4C, GW9662 also effectively blocked 15dPGJ<sub>2</sub>-mediated suppression of the relative collagen production (the percent of collagen production to total protein synthesis), indicating the selectivity of collagen synthesis inhibition by 15dPGJ<sub>2</sub> is also dependent on PPAR $\gamma$ . It was also important to note that WY14643 produced the inhibitory effects at the concentrations known to activate both PPAR $\alpha$  and  $\gamma$  (>100  $\mu$ M) but not at those that only activate PPAR $\alpha$  (<10  $\mu$ M); EC<sub>50</sub> for mouse PPAR $\alpha$  and  $\gamma$  are 0.6 and 30  $\mu$ M, respectively (see Ref. 34 for review). In addition, a synthetic PPAR $\alpha$ -selective ligand (GW9578) failed to inhibit HSC collagen synthesis (data not shown). Thus, the observed inhibition with WY14643 likely reflects a PPAR $\gamma$ -mediated effect.

**Effects of 15dPGJ<sub>2</sub> and WY14643 on HSC Activation Marker Genes**—To further examine the effects of PPAR ligands, mRNA expression of HSC activation marker genes was screened by semi-quantitative RT-PCR after treatment of the cells with 15dPGJ<sub>2</sub> and WY14643. 15dPGJ<sub>2</sub> (10  $\mu$ M) caused conspicuous and consistent suppression of  $\alpha$ 1(I) collagen and  $\alpha$ -SMA mRNA expression in HSC treated with or without TNF $\alpha$  (Fig. 5A). MCP-1 expression was also moderately inhibited by the treatment with 15dPGJ<sub>2</sub> (Fig. 5A). These inhibitory effects were not due to general and systematic suppression of the cellular functions, since MMP-3 and CD36 were induced by the same treatment (Fig. 5, A and B). Treatment with WY14643 (250  $\mu$ M) also reduced  $\alpha$ 1(I) collagen and  $\alpha$ -SMA mRNA levels (Fig. 5C). TNF $\alpha$ -induced MCP-1 mRNA expression was also suppressed by WY14643 (Fig. 5C). Interestingly, WY14643 did not induce MMP-3 expression but increased MMP-13 mRNA level (Fig. 5C). CD36 was not induced by WY14643 (data not shown). Thus, these findings demonstrate the following: 1) 15dPGJ<sub>2</sub> and WY14643 inhibit HSC collagen expression at the pretranslational level, 2) other HSC activation markers such as enhanced DNA synthesis, expression of  $\alpha$ -SMA and MCP-1, are also inhibited by the treatments, 3) different MMPs are induced by 15dPGJ<sub>2</sub> and WY14643, and 4) 15dPGJ<sub>2</sub> induces HSC expression of CD36, a scavenger receptor, whose promoter contains PPRE (43).

**Effects of 15dPGJ<sub>2</sub> and BRL49653 on Collagen Gene Promoter**—To further examine the mechanism underlying inhibition of HSC collagen gene expression by 15dPGJ<sub>2</sub> and BRL49653, we co-transfected HSC with an  $\alpha$ 1(I) collagen promoter-luciferase construct (pGLCOL2) and a PPAR $\gamma$  expression vector and exposed the cells to the respective ligand. As shown in Fig. 6, 15dPGJ<sub>2</sub> and BRL49653 inhibited the promoter activity by 60 and 50%, respectively. These results suggest that the demonstrated inhibition of HSC collagen expression with the PPAR $\gamma$  ligands is mediated at least in part via the transcriptional effects.

**Morphological Changes Induced by 15dPGJ<sub>2</sub>**—Since PPAR ligands inhibited biochemical changes that are characteristic of

$p < 0.01$ . C, the inhibitory effect on HSC collagen production by 15dPGJ<sub>2</sub> is PPAR $\gamma$ -dependent. A PPAR $\gamma$  antagonist (GW9662) was added 1 h before incubation with 15dPGJ<sub>2</sub> for 18 h. Note this antagonist eliminated the 15dPGJ<sub>2</sub>-mediated inhibition of collagen production by 75% (lower panel), supporting the role of PPAR $\gamma$  in this regulation. The upper panel depicts 15dPGJ<sub>2</sub> as selectively inhibiting collagen synthesis, as shown by a significant decrease in relative collagen production (the percent of collagen production to total protein production) and that this selective inhibition was abrogated by GW9662.



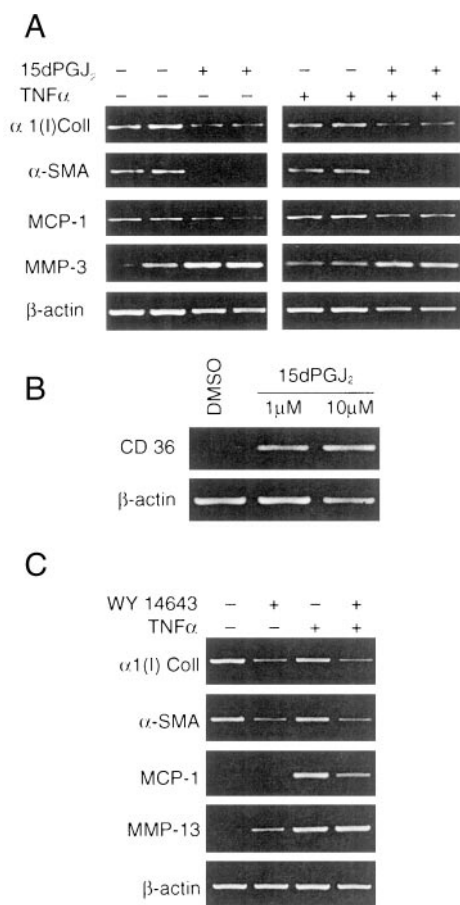


**FIG. 5. Suppression of activation marker genes in cultured HSC with 15dPGJ<sub>2</sub> or WY14643.** A, messenger RNA expression for  $\alpha 1(I)$  procollagen ( $\alpha 1(I)Coll$ ),  $\alpha$ -SMA, and MCP-1 is inhibited by 15dPGJ<sub>2</sub> (10  $\mu$ M), whereas MMP-3 was induced by the ligand in the 3–4-day-cultured HSC (left panel). The cells treated with TNF $\alpha$  responded similarly to 15dPGJ<sub>2</sub> (right panel). B, expression of CD36 was induced in 15dPGJ<sub>2</sub>-treated HSC as compared with the cells treated with a vehicle control (Me<sub>2</sub>SO (DMSO)). C, WY14643 (100  $\mu$ M) suppressed  $\alpha 1(I)$  procollagen and  $\alpha$ -SMA mRNA expression but induced MMP-13 expression by cultured HSC. DMSO, Me<sub>2</sub>SO.

HSC activation, we also examined whether 15dPGJ<sub>2</sub> or BRL49653 affected morphological features of HSC activation. Culture-activated HSC demonstrated a flattened spread shape, prominent actin stress fibers, and archetypal arrowhead-shaped focal adhesion complexes, as described previously (16). HSC treated with 10  $\mu$ M 15dPGJ<sub>2</sub> (Fig. 7) or 10  $\mu$ M BRL49653 (data not shown) appeared somewhat less spread-out and had mildly diminished stress fibers and focal adhesion complexes without any signs of cytotoxicity. These results suggest that the PPAR $\gamma$  ligands may modulate activation-associated alterations in the actin cytoskeleton and morphology of HSC.

**Culture Activation and TNF $\alpha$  Suppress PPAR $\gamma$  Expression, and 15dPGJ<sub>2</sub> Abrogates This Inhibition**—We then questioned whether culture-activated HSC also have reduced expression of PPAR $\gamma$  as in HSC from BDL animals. As shown in Fig. 8A, RT-PCR (30 cycles of amplification) of RNA freshly isolated and cultured HSC revealed a rapid decline in PPAR $\gamma$  expression in HSC cultured on plastic for 3 days, the time point when HSC began myofibroblastic activation. Suppressed PPAR $\gamma$  expression was sustained on day 7. However, the treatment of the 7-day cultured HSC with 15dPGJ<sub>2</sub> (10  $\mu$ M) for 18 h caused restoration of PPAR $\gamma$  expression (last lane), suggesting transcriptional induction of this gene containing functional PPRE. Next we questioned why PPAR $\gamma$  expression was suppressed in the *in vivo* activated HSC from BDL animals (Figs. 2 and 3).

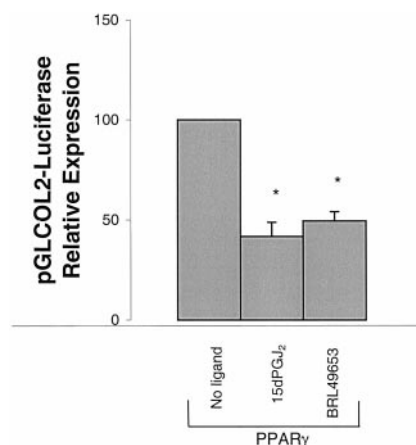


**FIG. 6. Inhibition of  $\alpha 1(I)$  collagen gene promoter with 15dPGJ<sub>2</sub> and BRL49653.** Cultured HSC after the first passage were co-transfected with an  $\alpha 1(I)$  collagen promoter and a PPAR $\gamma$  expression vector and exposed to 15dPGJ<sub>2</sub> (10  $\mu$ M) or BRL49653 (10  $\mu$ M). Luciferase activities were normalized by protein concentrations and expressed as the relative expression to that without ligand treatment. Note significant, 60 and 50%, reductions in the promoter activity caused by 15dPGJ<sub>2</sub> and BRL49653, respectively.

TNF $\alpha$  is known to inhibit PPAR $\gamma$  mRNA expression and expression of other adipocyte-specific genes in 3T3-L1 adipocytes (45). Expression of this cytokine is induced in liver injury including cholestatic liver injury (39). Furthermore, TNF $\alpha$  also appears to play a role in the early phase of HSC activation in liver fibrogenesis (46). Thus, we tested whether PPAR $\gamma$  mRNA expression was inhibited by TNF $\alpha$  and how 15dPGJ<sub>2</sub> affected this regulation in 3-day cultures of HSC. Using 35 cycles of PCR, PPAR $\gamma$  was sufficiently amplified to show a more distinct band in these cells (Fig. 8B, first and second lanes) as compared with Fig. 8A. TNF $\alpha$  inhibited basal mRNA expression of PPAR $\gamma$  (Fig. 8B, fifth and sixth lanes as compared with first and second lanes). However the concomitant treatment of the cells with 15dPGJ<sub>2</sub> abrogated this inhibition (seventh and eighth lanes). The same TNF $\alpha$  treatment did not result in apparent changes in PPAR $\alpha$  mRNA level, as assessed by the semi-quantitative RT-PCR (data not shown).

## DISCUSSION

This study demonstrated that PPAR $\gamma$  expression and PPRE binding were diminished in HSC as they underwent myofibroblastic activation in experimental cholestatic liver fibrosis in a somewhat analogous manner to transdifferentiation of 3T3-L1 adipocytes to fibroblasts. However, HSC were shown to lack expression of either adipocyte-specific PPAR $\gamma 2$  isoform (Fig. 1) or adipocyte-specific genes such as aP2, providing weak support to the hypothesis that HSC share the adipocyte phenotype. Furthermore, *in vivo* activation of HSC was also accompanied by reduced expression of PPAR $\alpha$ , a transcription factor mostly involved in regulation of genes encoding enzymes for fatty acid metabolism. Even though these findings only showed the association, our *in vitro* findings served as direct evidence for the regulatory role of PPAR in HSC activation. In culture-activated HSC, the ligands for PPAR $\gamma$  (15dPGJ<sub>2</sub>, BRL49653) and WY14643 at the concentrations that activate both PPAR $\alpha$  and  $\gamma$  consistently reversed biochemical changes that were characteristic of HSC activation. Since 15dPGJ<sub>2</sub> is known to have PPAR-independent effects (47, 48), we tested whether the suppressive effect of 15dPGJ<sub>2</sub> on HSC collagen synthesis was mediated via PPAR $\gamma$  by using an irreversible PPAR $\gamma$  ligand (GW9662), which works as an effective antagonist for PPAR $\gamma$

<sup>2</sup> T. Miyahara, S. Xiong, and H. Tsukamoto, unpublished data.

**FIG. 7. Morphological changes in cultured HSC exposed to 15dPGJ<sub>2</sub>.** Representative differential interference contrast and fluorescent images of the 7-day-cultured HSC exposed to the carrier (A, B, and C) or 10  $\mu$ M (D, E, and F) 15dPGJ<sub>2</sub>. Differential interference contrast images are presented in the left column (A and D). Cells stained for actin stress fibers are displayed in the middle column (B and E); cells stained for focal adhesion complexes are displayed in the right column (C and F).

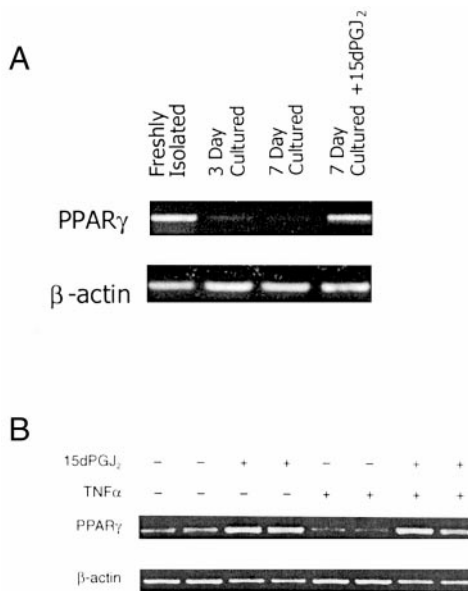
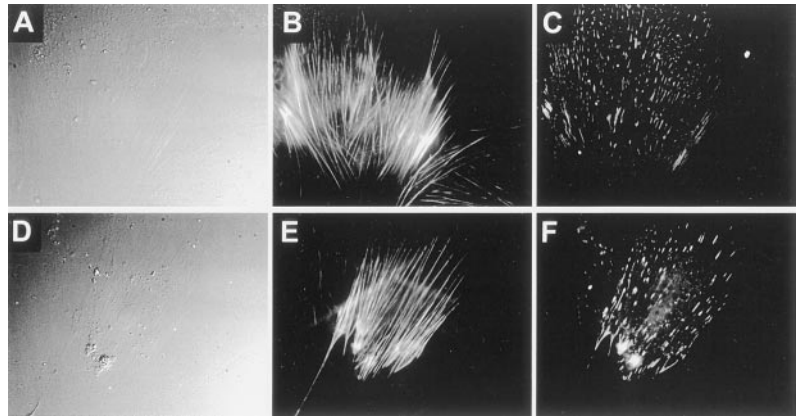


**FIG. 8. Culture activation and TNF $\alpha$  suppress PPAR $\gamma$  mRNA expression by HSC and 15dPGJ<sub>2</sub> abrogates this effect.** A, RT-PCR analysis (30 cycles of amplification) of RNA from freshly isolated and cultured HSC demonstrates a rapid decline in PPAR $\gamma$  expression in culture for 3 days and sustained suppression of the gene on day 7. The treatment of the 7-day-cultured HSC with 15dPGJ<sub>2</sub> (10  $\mu$ M) for 18 h caused restoration at PPAR $\gamma$  expression (last lane). B, RT-PCR analysis (35 cycles of amplification) of RNA from the 3–4-day-cultured HSC exposed to TNF $\alpha$  without or with 15dPGJ<sub>2</sub>. The treatment of the 3–4-day HSC cultures with TNF $\alpha$  (10 ng/ml) further inhibited PPAR $\gamma$  expression (lane 5 and 6). However, the concomitant treatment of the cells with 15dPGJ<sub>2</sub> abrogated this inhibition (lanes 7 and 8).

(33, 34). Indeed, GW9662 eliminated the 15dPGJ<sub>2</sub>-mediated inhibition by 70%, supporting the involvement of PPAR $\gamma$  in this effect. Besides collagen synthesis, the inhibitory effects by the ligands were seen on many key parameters of HSC activation, including DNA synthesis, mRNA expression for  $\alpha$ 1(I) collagen,  $\alpha$ -SMA, and MCP-1, and collagen promoter activity. We carefully ruled out the potential cytotoxic effects of the ligands by performing the sensitive staining for necrosis and apoptosis. The concentrations of the ligands used caused no cell death. We also identified the genes such as MMPs and CD36 that were induced in cultured HSC treated with the ligands, supporting the fact that the cells were not under cytotoxic conditions. Differential effects were seen with 15dPGJ<sub>2</sub> and WY14643 on induction of MMP-3 and MMP-13. The reason for this difference is unknown at the present time, and induction at the protein level was not ascertained in this study. However, if the observed induction of MMP-13 is confirmed at the protein and activity levels, this indicates that WY14643 has dual inhibitory

effects on liver fibrogenesis via inhibition of collagen production and stimulation of matrix degradation. Interpretation of the induced MMP-3 by 15dPGJ<sub>2</sub> is more complicated since it may signify the initiation of degradation of the normal matrix in the perisinusoidal space while it may also serve as an anti-fibrotic effect via degradation of increased deposition of MMP-3 sensitive matrix components in liver fibrosis.

Induction of CD36 by 15dPGJ<sub>2</sub> is intriguing. CD36 is a membrane glycoprotein expressed by macrophages, adipocytes, endothelial cells, smooth muscle cells, and many other cell types that participates in uptake of oxidized low density lipoprotein (43), long chain fatty acids (49), thrombospondin-1 binding (50), as well as phagocytosis of apoptotic cells (51). Oxidized low density lipoprotein is considered to contain PPAR $\gamma$  ligands, and once internalized, they may serve to activate PPAR $\gamma$ -RXR to further induce CD36 (43) and to inhibit the activated phenotype of HSC. On the other hand, this inhibition may also be opposed by the effects by lipid peroxides and aldehydes liberated from oxidized low density lipoprotein, which are known to induce oxidative stress and to signal for activation of HSC (52). At the same time, induction of CD36 may enhance uptake of long chain fatty acids, potentially promoting lipid storage. The functional consequence of PPAR $\gamma$  ligand-induced up-regulation of CD36 in HSC needs to be addressed in future studies by performing careful kinetic studies on the effects of oxidized low density lipoprotein and unoxidized fatty acids.

The present study demonstrated that PPAR $\gamma$  ligands inhibited collagen gene expression at least in part through inhibition of collagen gene promoter activity. The mechanisms of this transcriptional inhibition are unknown. However, a PPAR $\alpha$  ligand (WY14643) but not a PPAR $\gamma$  ligand (BRL49653) was recently shown to inhibit interleukin-1-induced expression of interleukin-6 and COX-2 by human smooth muscle cells via repression of NF- $\kappa$ B (44). Similar negative cross-coupling of NF- $\kappa$ B, AP-1, or STAT activities in monocyte/macrophage cell lines has been demonstrated by 15dPGJ<sub>2</sub> and BRL49653 (42). Thus, the observed inhibitory effects of PPAR $\gamma$  ligands in the present study may also be mediated via PPAR $\gamma$ -mediated antagonism on transcription factors that drive the collagen gene promoter. Alternatively, the antagonism may be mediated by the effects of the ligands on the upstream-signaling mechanisms leading to the observed repression of the collagen gene promoter. In fact, troglitazone, a synthetic PPAR $\gamma$  ligand, inhibits mitogen-activated protein kinase activity when it suppresses DNA synthesis and migration of vascular smooth muscle cells (53). In a recent study testing PPAR ligands on colonic epithelial cells, 15dPGJ<sub>2</sub> treatment was shown to prevent interleukin-1 $\beta$ -induced I $\kappa$ B- $\alpha$  degradation, suggesting the upstream inhibitory effect of the ligand (54). In fact, this effect may be due to direct inhibition of I $\kappa$ Bkinase independent of

PPAR $\gamma$  (47, 48). Future studies will characterize locations of upstream signaling affected by the PPAR $\gamma$  ligands as well as the elements within the promoter that are responsible for the repressive effects of the ligands.

Our results also provided the *in vitro* evidence for the potential role of TNF $\alpha$  in suppression of PPAR $\gamma$  expression in HSC as we observed *in vivo*. The similar effect was previously shown in 3T3-L1 adipocytes, in which a time- and concentration-dependent decrease in PPAR $\gamma$  mRNA expression was observed after TNF $\alpha$  treatment, the effect considered as the biochemical basis for anti-adipogenic effects of TNF $\alpha$  (45). It remains to be tested whether TNF $\alpha$  is indeed responsible for PPAR $\gamma$  repression observed in HSC in cholestatic liver fibrosis. It should be noted that growth factors such as epidermal growth factor and platelet-derived growth factor are also capable of inhibiting PPAR $\gamma$  expression via mitogen-activated protein kinase-mediated phosphorylation of PPAR $\gamma$  (55). Since both TGF- $\alpha$  and platelet-derived growth factor are implicated in HSC activation as autocrine and paracrine mitogens (1, 8, 46), we cannot rule out the role of these growth factors in PPAR $\gamma$  inhibition *in vivo*. Remarkably, the concomitant treatment of HSC with 15dPGJ<sub>2</sub> completely abrogated the TNF $\alpha$ -induced suppressive effect on PPAR $\gamma$ . This ligand also restored PPAR $\gamma$  mRNA expression in culture-activated HSC that showed a rather rapid decline in expression of this transcription factor. In fact, we believe this induction by 15dPGJ<sub>2</sub> facilitated the responsiveness of cultured HSC to the ligand, as demonstrated by suppressed expression of activation marker genes (collagen,  $\alpha$ -SMA, MCP-1) and induction of CD36 and MMPs. These findings further suggest that 15dPGJ<sub>2</sub> and other PPAR $\gamma$  ligands may serve as effective anti-fibrotic agents, since it normalizes PPAR $\gamma$  expression while suppressing the activation marker genes at the same time. Alternatively, we could interpret that the latter effect is a consequence of the former effect. The normalized level of endogenous PPAR $\gamma$  likely transduces better anti-fibrotic effects of the endogenous or exogenous ligands, especially when the HSC content of RXR and 9-*cis* RA, the active partner/ligand for PPAR $\gamma$ , is depleted as in liver fibrosis (22). *In vivo* effects of PPAR $\gamma$  ligands on development and progression of liver fibrosis are currently being investigated.

## REFERENCES

- Friedman, S. L. (1993) *N. Engl. J. Med.* **328**, 1828–1835
- Bissell, D. M. (1990) *Semin. Liver Dis.* **10**, 3–4
- Hautekeer, M. L., and Geerts, A. (1997) *Virchows Arch.* **430**, 195–207
- Friedman, S. L., Wei, S., and Blaner, W. S. (1993) *Am. J. Physiol.* **264**, G947–G952
- Tsukamoto, H., Cheng, S., and Blaner, W. S. (1996) *Am. J. Physiol.* **270**, G581–G586
- Poulos, J. E., Weber, J. D., Bellezzo, J. M., Di Bisceglie, A. M., Britton, R. S., Bacon, B. R., and Baldassare, J. J. (1997) *Am. J. Physiol.* **273**, G804–G811
- Carloni, V., Romanelli, R. G., Pinzani, M., Laffi, G., and Gentilini, P. (1997) *Gastroenterology* **112**, 522–531
- Bachem, M. G., Meyer, D., Melchior, R., Sell, K. M., and Gressner, A. M. (1992) *J. Clin. Invest.* **89**, 19–27
- Matsuoka, M., Zhang, M. Y., and Tsukamoto, H. (1990) *Hepatology* **11**, 173–182
- Maher, J. J., and McGuire, R. F. (1990) *J. Clin. Invest.* **86**, 1641–1648
- Nakatsukasa, H., Nagy, P., Evarts, R. P., Hsia, C. C., Marsden, E., and Thorgeirsson, S. S. (1990) *J. Clin. Invest.* **85**, 1833–1843
- Iredale, J. P., Goddard, S., Murphy, G., Benyon, R. C., and Arthur, M. J. (1995) *Clin. Sci. (Lond.)* **89**, 75–81
- Rockey, D. C., Boyles, J. K., Gabbiani, G., and Friedman, S. L. (1992) *J. Submicrosc. Cytol. Pathol.* **24**, 193–203
- Rockey, D. C., Housset, C. N., and Friedman, S. L. (1993) *J. Clin. Invest.* **92**, 1795–1804
- Rockey, D. C., and Chung, J. J. (1996) *J. Clin. Invest.* **98**, 1381–1388
- Yee, H. F., Jr. (1998) *Hepatology* **28**, 843–850
- Wang, S. C., Ohata, M., Schrum, L., Rippe, R. A., and Tsukamoto, H. (1998) *J. Biol. Chem.* **273**, 302–308
- Friedman, S. L., Yamasaki, G., and Wong, L. (1994) *J. Biol. Chem.* **269**, 10551–10558
- Wong, L., Yamasaki, G., Johnson, R. J., and Friedman, S. L. (1994) *J. Clin. Invest.* **94**, 1563–1569
- Qi, Z., Atsuchi, N., Ooshima, A., Takeshita, A., and Ueno, H. (1999) *Proc. Natl. Acad. Sci. U. S. A.* **96**, 2345–2349
- Kim, Y., Ratziu, V., Choi, S. G., Lalazar, A., Theiss, G., Dang, Q., Kim, S. J., and Friedman, S. L. (1998) *J. Biol. Chem.* **273**, 33750–33758
- Ohata, M., Lin, M., Satre, M., and Tsukamoto, H. (1997) *Am. J. Physiol.* **272**, G589–G596
- Salbert, G., Fanjul, A., Piedrafita, F. J., Lu, X. P., Kim, S. J., Tran, P., and Pfahl, M. (1993) *Mol. Endocrinol.* **7**, 1347–1356
- Pan, L., Eckhoff, C., and Brinckerhoff, C. E. (1995) *J. Cell. Biochem.* **57**, 575–589
- Pektovich, M., Brand, N. J., Krust, A., and Chambon, P. (1987) *Nature* **330**, 444–450
- Davis, B. H., Kramer, R. T., and Davidson, N. O. (1990) *J. Clin. Invest.* **86**, 2062–2070
- Okuno, M., Moriwaki, H., Imai, S., Muto, Y., Kawada, N., Suzuki, Y., and Kojima, S. (1997) *Hepatology* **26**, 913–921
- Imai, S., Okuno, M., Moriwaki, H., Muto, Y., Murakami, K., Shudo, K., Suzuki, Y., and Kojima, S. (1997) *FEBS Lett.* **41**, 102–106
- Hellemans, K., Grinko, I., Rombouts, K., Schuppan, D., and Geerts, A. (1999) *Gut* **45**, 134–142
- Mangelsdorf, D. J., Umesono, K., and Evans, R. M. (1994) in *The Retinoids: Biology, Chemistry, and Medicine* (Sporn, M. B., Roberts, A. B., and Goodman, D. S., eds), Raven Press, Ltd., New York, 319–349
- Potter, J. J., Womack, L., Mezey, E., and Anania, F. A. (1998) *Biochem. Cell Biol.* **244**, 178–182
- Spiegelman, B. M., and Flier, J. S. (1996) *Cell* **87**, 377–389
- Huang, J. T., Welch, J. S., Ricote, M., Binder, C. J., Willson, T. M., Kelly, C., Witztum, J. L., Funk, C. D., Conrad, D., and Glass, C. K. (1999) *Nature* **400**, 378–382
- Willson, T. M., Brown, P. J., Sternbach, D. D., and Henke, B. R. (2000) *J. Med. Chem.* **43**, 527–550
- Chomczynski, P., and Sacchi, N. (1987) *Anal. Biochem.* **162**, 156–159
- Schreiber, E., Matthias, P., Muller, M. M., and Schaffner, W. (1989) *Nucleic Acids Res.* **17**, 6419
- Vidal-Puig, A., Jimenez-Linan, M., Lowell, B. B., Hamann, A., Hu, E., Spiegelman, B., Flier, J. S., and Moller, D. E. (1996) *J. Clin. Invest.* **97**, 2553–2561
- Juge-Aubry, C., Pernin, A., Favez, T., Burger, A. G., Wahli, W., Meier, C. A., and Desvergne, B. (1997) *J. Biol. Chem.* **272**, 25252–25259
- Lin, M., Rippe, R. A., Niemela, O., Brittenham, G., and Tsukamoto, H. (1997) *Am. J. Physiol.* **272**, G1355–G1364
- Rippe, R. A., Almounajed, G., and Brenner, D. A. (1995) *Hepatology* **22**, 241–251
- Devchand, P. R., Keller, H., Peters, J. M., Vazquez, M., Gonzalez, F. J., and Wahli, W. (1996) *Nature* **384**, 39–43
- Ricote, M., Li, A. C., Willson, T. M., Kelly, C. J., and Glass, C. K. (1998) *Nature* **391**, 79–82
- Tontonoz, P., Nagy, L., Alvarez, J. G., Thomazy, V. A., and Evans, R. M. (1998) *Cell* **93**, 241–252
- Staels, B., Koenig, W., Habib, A., Merval, R., Lebreton, M., Torra, I. P., Delerive, P., Fadel, A., Chinetti, G., Fruchart, J. C., Najib, J., Maclouf, J., and Tedgui, A. (1998) *Nature* **393**, 790–793
- Zhang, B., Berger, J., Hu, E., Szalkowski, D., White-Carrington, S., Spiegelman, B. M., and Moller, D. E. (1996) *Mol. Endocrinol.* **10**, 1457–1466
- Tsukamoto, H. (1999) *Alcohol Clin. Exp. Res.* **23**, 911–916
- Rossi, A., Kapahi, P., Natoli, G., Takahashi, T., Chen, Y., Karin, M., and Santoro, M. G. (2000) *Nature* **403**, 103–108
- Castrillo, A., Diaz-Guerra, M. J., Hortelano, S., Martin-Sanz, P., and Bosca, L. (2000) *Mol. Cell. Biol.* **20**, 1692–1698
- Abumrad, N. A., el Maghrabi, M. R., Amri, E. Z., Lopez, E., and Grimaldi, P. A. (1993) *J. Biol. Chem.* **268**, 17665–17668
- Dawson, D. W., Pearce, S. F., Zhong, R., Silverstein, R. L., Frazier, W. A., and Bouck, N. P. (1997) *J. Cell Biol.* **138**, 707–717
- Fadok, V. A., Warner, M. L., Bratton, D. L., and Henson, P. M. (1998) *J. Immunol.* **161**, 6250–6257
- Parola, M., Robino, G., Marra, F., Pinzani, M., Bellomo, G., Leonarduzzi, G., Chiarugi, P., Camandola, S., Poli, G., Waeg, G., Gentilini, P., and Dianzani, M. U. (1998) *J. Clin. Invest.* **102**, 1942–1950
- Graf, K., Xi, X. P., Hsueh, W. A., and Law, R. E. (1997) *FEBS Lett.* **400**, 119–121
- Su, C. G., Wen, X., Bailey, S. T., Jiang, W., Rangwala, S. M., Keilbaugh, S. A., Flanagan, A., Murthy, S., Lazar, M. A., and Wu, G. D. (1999) *J. Clin. Invest.* **104**, 383–389
- Camp, H. S., and Tafuri, S. R. (1997) *J. Biol. Chem.* **272**, 10811–10816